Journal of Applied Polymer Science

Flexographic Printed Carbon Nanotubes on Polycarbonate Films Yielding High Heating Rates

Thomas Fischer,[1] Nora Wetzold,[2] Lothar Kroll,[1] Arved Hübler[2]
[1]Institute of Lightweight Structures, Chemnitz University of Technology, Chemnitz 09126, Germany
[2]Institute for Print and Media Technology, Chemnitz University of Technology, Chemnitz 09126, Germany
Correspondence to: T. Fischer (E-mail: thomas.fischer@mb.tu-chemnitz.de)

ABSTRACT: Carbon nanotube (CNT) formulations based on commercially available aqueous dispersions were printed using flexographic printing on a polycarbonate film which was provided with a polyethyleneimine-based primer layer to improve the wetting and adhesion properties. Depending on the formulation, the structured CNT layers (35 mm × 50 mm) show heating rates of up to 14 K/s during resistive heating (applied voltage of 12 V) in the temperature range from room temperature to 70°C. The recording of temperature–time curves was carried out by means of an infrared camera system. The cooling largely depends on the substrate and its heat capacity as well as on environmental conditions, and could be actively supported and/or regulated. The formulations of different solid contents were described in terms of viscosity and surface tension while the printed layers were characterized regarding the mass load per area, sheet resistance, electrical power effective during resistive heating, and the layer morphology. © 2013 Wiley Periodicals, Inc. J. Appl. Polym. Sci. 129: 2112–2120, 2013

KEYWORDS: applications; films; nanotubes; graphene ; fullerenes

Received 27 September 2012; accepted 10 December 2012; published online 13 January 2013
DOI: 10.1002/app.38924

INTRODUCTION

For the application of carbon nanotubes (CNTs) on various substrates, printing techniques have become more frequently the preferred technologies.[1] Printing processes for the application of CNT layers, as described in the literature, are screen printing,[2,3] ink jet printing,[4–6] gravure printing,[7] and aerosol jet technology.[8]

In recent years, intensive research has been done in the field of (full area or structured) coating of flexible surfaces with functional materials in many parts of the world. Printed electronics, which aims at realizing low-cost solutions for manifold functionalities, take a leading role here. Conventional mass-printing methods, like flexographic printing, have the potential to realize functional layers in continuous roll-to-roll (R2R) processes. In comparison to other conventional printing methods, printing forms for flexography can be fabricated in a simple and cost-efficient way. Ink transfer requires relatively low contact pressure. Therefore, it is well-suited for research activities in the laboratory. In production, web widths of several meters and printing speeds of up to 720 m/min are possible. Today, many research institutions have modular printing machines with a broad range of web widths, printing methods, and additional equipment. Therefore, very specific R&D activities are possible, covering the whole spectrum from laboratory to industry scale while keeping specific process parameters constant and avoiding technology leaps in the course of scale-up steps.

Commercially available aqueous CNT dispersions provide the ideal basis for adaptation to R2R mass printing processes, such as flexographic printing.[9,10]

Electrical resistance, as one of the main characteristics for the heating behavior, can be adjusted by regulating the layer thickness, i.e. by the number of multiple prints. The semi-finished products of substrate and CNT structures produced by printing can be pre-assembled and e.g. integrated into composite parts for a further specific functionalization.

The first results for flexographic printing of CNT dispersions on a textile substrate (multi-filament fleece) and paper were published in 2011.[11] The properties of the printed layers, such as the dependence of the layer resistance on the surface mass and the achievable electrical power for heating relative to a printed surface segment, were treated. An aqueous dispersion from Future Carbon GmbH, Germany served as the basis for the printed CNT formulations.

Printing as an application process for CNT-based inks is introduced in detail in previous publications.[2,5–8,12]

Table 1. CNT Formulations

AQ12	AQ13	AQ35	FC23
Basis:	Basis:	Basis:	Basis:
Aquacyl 1 wt % CNT	Aquacyl 1 wt % CNT	Aquacyl 3 wt % CNT	CarboDis 2 wt % CNT
Formulation:	Formulation:	Formulation:	Formulation:
2 wt % CNT	3 wt % CNT	3.5 wt % CNT	3 wt % CNT

A combination of flexographic printing, as an application process for printable formulations based on aqueous CNT dispersions, with film substrates has not yet been described.

A potential application of CNT surfaces, also discussed in the literature,[13,14] is as a surface heating element utilizing resistive heating. If in addition to functioning as a heating element the CNT surfaces should also be transparent, then single-walled carbon nanotubes (SWCNTs) have to be used as described in a previous study.[15] Multi-walled carbon nanotubes (MWCNTs), consisting of several nanotubes nested within one another, can be produced using a simpler and therefore cheaper technology; however, they have a higher defect density compared to SWCNT. Mechanical and electrical properties of MWCNTs may vary within a wide range and are inferior to those of SWCNTs. Large differences between the theoretical and experimentally determined values for individual CNTs regarding the thermal conductivity and the values of randomly arranged CNT layers are mentioned in Ref. 16. It is clear that the properties of disordered CNT networks depend on many factors. Worth mentioning are the type of CNTs, their aspect ratio, the grade of contamination, the type and number of defects, and the functionalization. If the CNTs are applied from a dispersion (ink) to a substrate surface, it is necessary to take into account the surface properties of the substrate and the composition of the dispersion (additives, binding agents, and dispersants). In addition, the influence of the application process parameters and the ambient conditions must also be considered. Temperature, humidity, pressure, relative velocity, and contact surfaces can be mentioned here as examples.

Flat heating elements are widely used, e.g. for temperature control in microfluidic components. In the literature, the polymerase chain reaction (PCR) in lab-on chip applications with its three-step temperature cycle is discussed in this context. This cycle basically comprises the steps of heating (90–95°C), cooling (50°C), and heating (60–70°C).[17–19] Depending on the heating principle, achievable heating rates of between 20 and 65 K/s are mentioned. Heating rates from about 10 K/s can be regarded as a minimum requirement.[18–21] Therefore, a great potential for low-cost applications can be unleashed if CNT structures can be implemented using a mass printing process, such as flexographic printing.

In the literature, polycarbonate (PC) is, for instance, used as carrier material for lab-on-chip systems. Its good mechanical properties, high stability, rigidity, impact resistance, hardness, and precise mold surface reproduction accuracy predestine PC for very small precision devices, which can be fabricated by means of batch production methods, like micro-injection molding. The possible functionalization of surfaces of PC devices, which have been fabricated by means of injection-molding, with printed nanomaterial layers considerably, extends the property spectrum of PC devices. The combination of the highly productive batch production methods printing and injection-molding promises a high potential concerning minimization of production time and improvement if material and energy efficiency.[22,23]

In addition, PC increasingly plays an important role in the field of electromobility. The polymeric material is used for glazing. In comparison to glass it has a much higher flexibility, greater freedom of design, better heat insulation, and lower weight. In electric vehicles, the battery has to provide the energy for interior heating. The passive effectiveness of PC with its good heat insulation properties can be supported by active surface elements at devices like column coverings, glazing segments, and battery housings. Possible are printed CNT layers that can be integrated into the light-weight structures. Especially in winter times, for instance, pre-heating of relevant surfaces can be realized while the battery is charging.[24]

MATERIALS AND METHODS

Materials

This article describes the use of aqueous dispersions adapted to flexographic printing from Future Carbon GmbH (FC formulations), Germany and Nanocyl SA (AQ formulations), Belgium. Substrates for comparative studies are plastic films made of PC. To improve the wetting behavior of formulations on the PC substrate, a primer layer on the base of polyethyleneimine was formed by a doctor blade. The main components of aqueous dispersions are MWCNTs. For the experiments of flexographic ink formulations, the dispersion CarboDis TN with a CNT content of 2 wt % has been chosen by Future Carbon GmbH. TN denotes the dispersion type with electrically neutral surfactant (2 wt %).

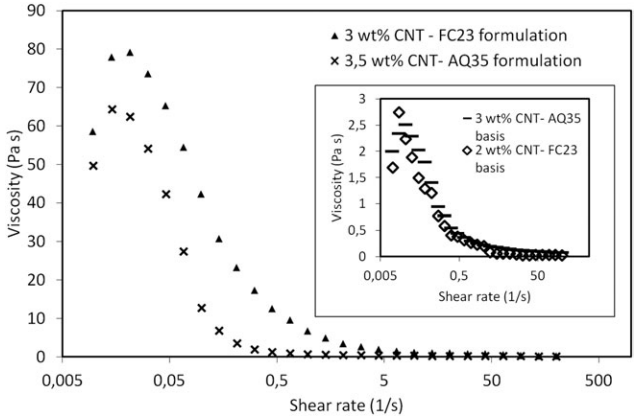

Figure 1. Flow curves of CNT formulations.

Applied Polymer SCIENCE

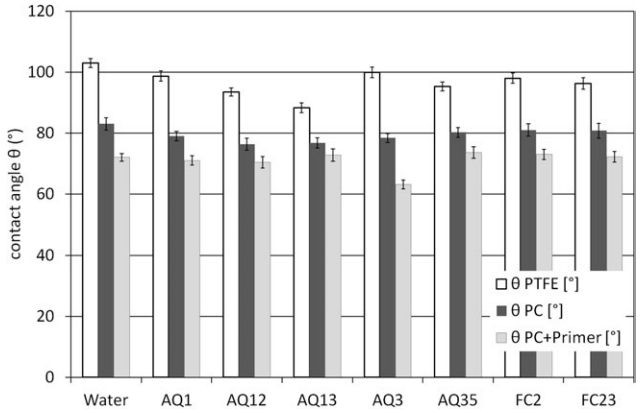

Figure 2. Contact angles of CNT formulations on a non-polar PTFE surface.

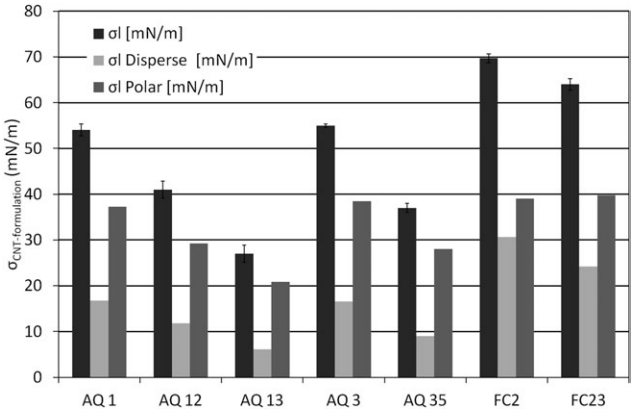

Figure 3. Surface tension of CNT formulations.

According to Future Carbon, the dynamic viscosity is less than 100 mPa s due to a multistage dispersing process.[25] The dispersions Aquacyl with 1 and 3 wt % CNTs from the company Nanocyl S.A. were used as the initial product for the formulation. According to the manufacturer's specification, the proportion of dispersant was <5 wt %.[26]

Methods

Viscosity. For determining the viscosity of chosen CNT dispersions and formulations, the Physica MCR301 rheometer, Application RHEOPLUS/32 V3.40 with the measuring system PP25-SN24213 d = 1mm was used. The measuring profile of the rotation test included a logarithmic acquisition of values with $d\gamma/dt = 0.01\ldots200$ 1/s.

Surface Energy, Prediction of Wetting Behavior. The surface tension of CNT dispersions was determined using the pendant drop method with the video-based optical contact angle and drop shape measuring system OCA 20 from dataphysics, Germany. The calculation of total surface tension according to Owens, Wendt, Kaelble, and Rabel was performed using the software of the measuring system.[27] The contact angle of the CNT formulations on the PC film substrate and polytetrafluoroethylene (PTFE) could be captured by means of the system-integrated camera. By determining the contact angle of the formulations on a PTFE surface (substrate with only disperse fraction of the surface energy), the disperse fraction can be calculated using the method according to Owens, Wendt, Kaelble and Rabel:

$$\sigma_l^D = \frac{1}{4}\frac{\sigma_l^2}{\sigma_s^D}(1+\cos\theta)^2 \qquad (1)$$

For characterizing the surface energy of the substrate, the sessile drop method in combination with an evaluation according to Owens, Wendt, Kaelble, and Rabel was used. The wetting behavior was illustrated by a wetting curve (wetting envelope). In a diagram with the polar and disperse fraction applied to the axes, wetting curves for different contact angles can be shown. If the surface tension values of a formulation are below the curve, a favorable wetting behavior (depending on the contact angle of the curve completely or partially wetting) can be expected. The wetting envelopes presented here were calculated on the basis of correlations described in Ref. 28.

Table 2. Surface Energies of the Substrates

	σ_s (mN/m)	σ^d (mN/m)	σ^p (mN/m)
PC + Primer	44.65	31.39	13.26
PC	39.22	36.37	2.85
PTFE	19.1	18.6	0.5

Printing. Printing tests were carried out on the flexographic test printing press FlexiProof 100-630 of Erichsen, Germany. Using a print layout in the form of areas with dimensions of 35 mm × 50 mm, 40 mm × 60 mm, and 50 mm × 70 mm, the CNT dispersion was transferred onto the substrate by means of a printing plate (DuPont Cyrel DPN) with a thickness of 1.7 mm. The ceramic anilox roller used had a scooping capacity of 25 cm^3/m^2 and the printing speed was 50 m/min. The CNT layer consisted of 20 individual layers.

Sheet Resistance. For measuring the sheet resistance of printed CNT films, an experimental setup for 4-point measurement with Keithley SourceMeter 6400 was used.

Mass of the Printed Layer. The mass parameters were determined by weighing the samples using an AX200 analytical balance.

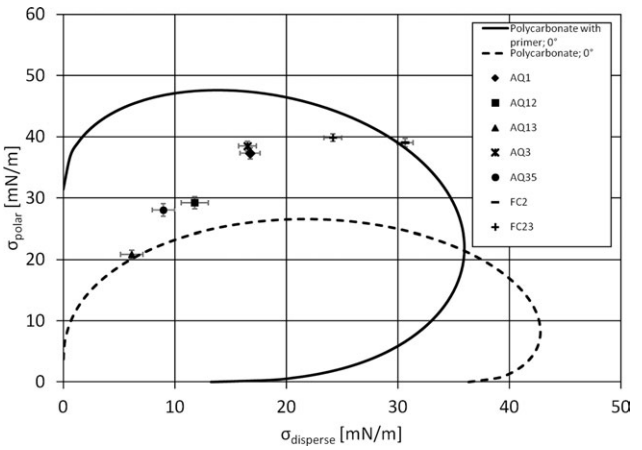

Figure 4. Wetting envelope; CNT formulations on PC film substrate.

SEM. For the SEM images of CNT films a high-resolution FE-SEM (field emission scanning electron microscope) Supra 60-32-10 from Zeiss was used.

Thermography. A CEDIP-IRT system with JAD-FPA camera with an upper temperature limit of 75°C was used for recording the temperature–time curves of printed CNT films.

CEDIP-IRT-system with JADE-FPA-camera:

- InSb-chip 320 × 240 pixel (30 μm × 30 μm)
- $\lambda^{MWIR} = 3.6–5.1\ \mu$m

objective: MW 5 mm 2.0 JADE0.

Ink Preparation. The formulations indicated in Table I were used as printing materials. CNT formulations AQ13 and AQ12

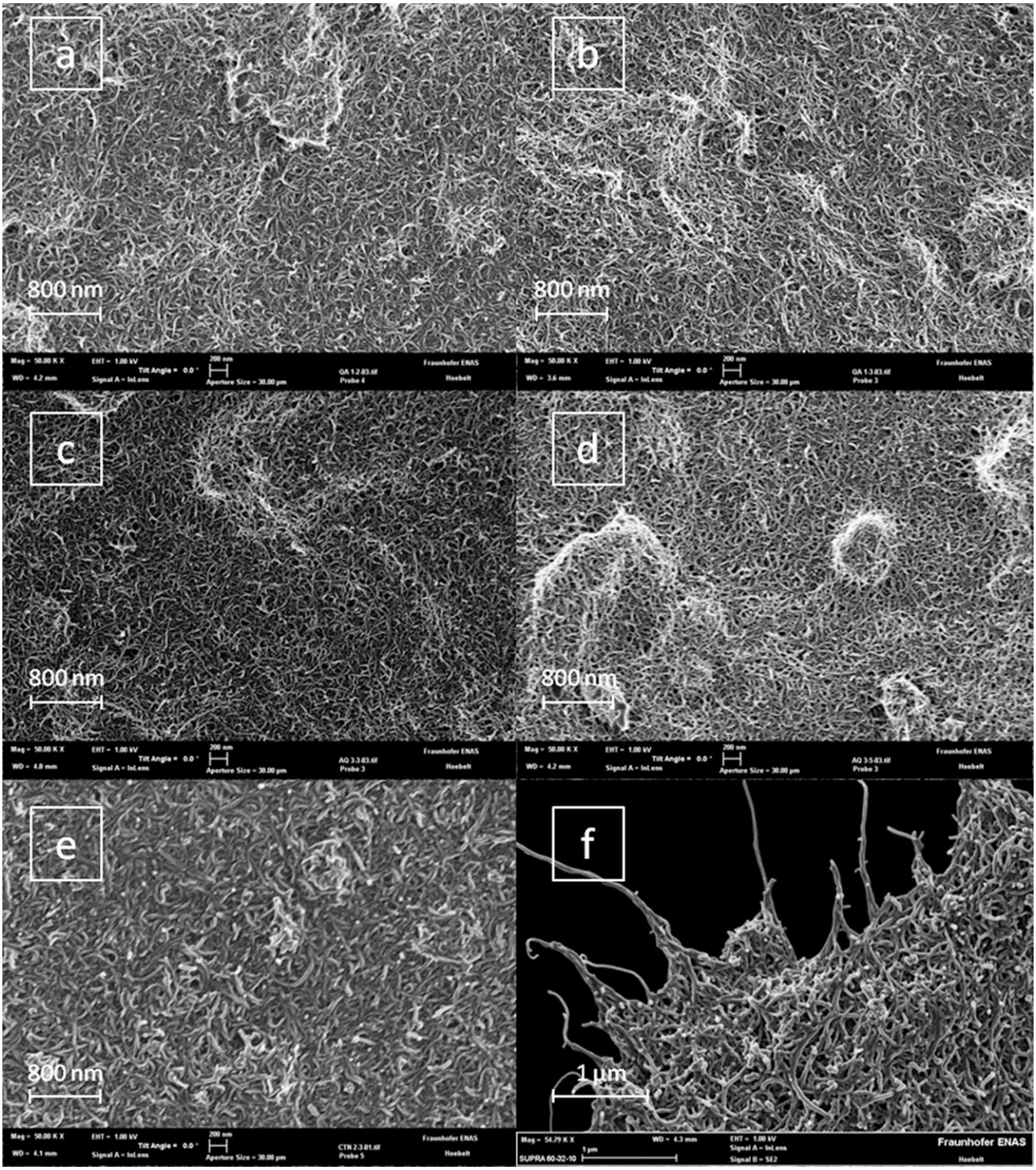

Figure 5. SEM images of printed CNT layers on PC film substrate; (a) AQ12, (b) AQ13, (c) AQ3, (d)AQ35, (e) FC23, (f) AQ3 edge of a layer.

Applied Polymer SCIENCE

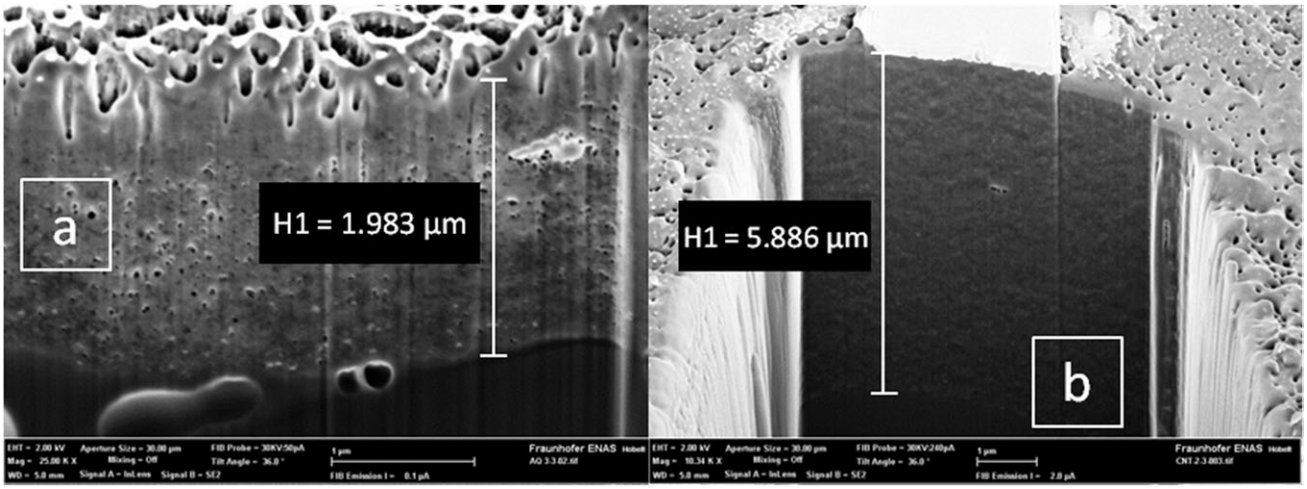

Figure 6. SEM-focused ion beam (FIB) images of (a) AQ3 layer and (b) FC23 layer.

with 2 resp. 3 wt % CNT were prepared on the basis of Nanocyl product Aquacyl with 1 wt% CNT and the variant AQ35 with 3.5 wt % CNT was developed on the basis of Aquacyl with 3 wt % CNT in the course of the formulation. The basis for the sample FC23 with 3 wt % CNT was the product CarboDis TN with 2 wt % CNT. The initial dispersions Aquacyl 1 wt % CNT and CNT CarboDis 2 wt % were not optimum for the printing process when used in a non-modified condition. During the preliminary experiments, it was not possible to achieve a sufficient transfer of printing material for a homogeneous formation of multilayer coatings.

Dispersion Measurements

Viscosity. Flow curves of selected formulations according to the CSR mode (controlled shear rate test) are shown in Figure 1. As expected, the curves showed a typical shear thinning behavior of dispersions. In comparison, the dispersions formulated by this group (i.e., by adjusting the batch formulation so that the solid content was increased at a shear rate of between 0.01 and 1 s^{-1}) showed higher viscosity values than the initial dispersions. The flow curves of the formulated dispersions are characterized by a so-called transient viscosity hill. The latter indicates the increase of transient effects due to the formulation process. Time-dependent interactions with surfaces of the measuring system, orientation of particles, change of shape, and dissolution of agglomerates cannot be fully compensated by increasing the measurement point duration. A homogeneous and nearly identical for all formulations curve shape at shear rates of >5 s^{-1} provided good conditions for the flexographic printability in terms of the rheological behavior.

The flow curves of different formulations allow one more statement. The two dispersions of the manufacturers Future Carbon and Nanocyl show nearly the same behavior after the adaptation to the printing process. The relative increase of the polymer portion and the associated change of viscosity have no significant effect on the curve shape despite the different initial formulations. It is therefore assumed that the polymeric binder systems are very similar.

Contact Angle–Surface Tension/Energy–Wetting Envelope. The contact angles of the CNT formulations were determined on an untreated PC film, on a PC film provided with a primer, and on a PTFE film. The fact that the contact angle on the PTFE film showed the highest values while the contact angle on the PC film treated with a primer showed the lowest ones applied to all formulations (see Figure 2). The reason for this is the surface

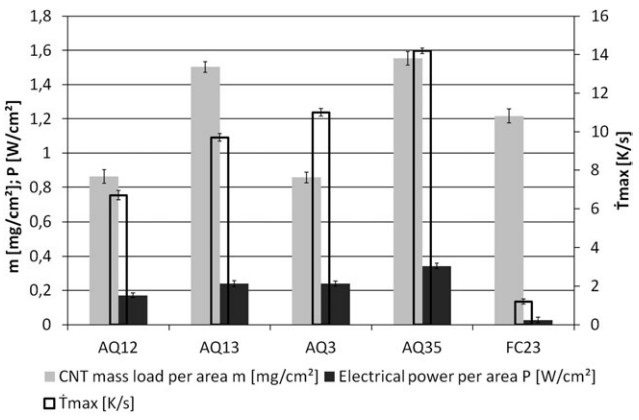

Figure 7. Mass load per area; electrical power, maximal heating rate of printed CNT layers.

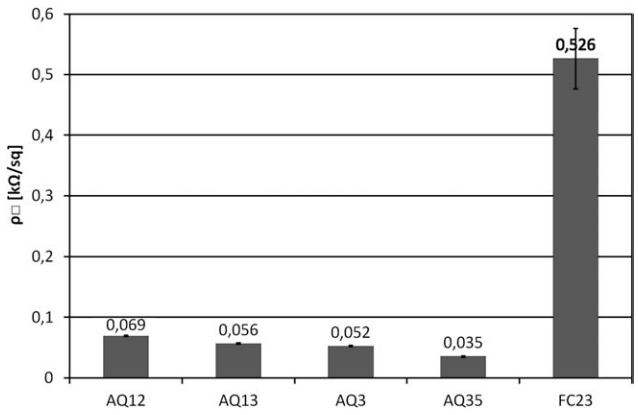

Figure 8. Sheet resistance of printed CNT layers.

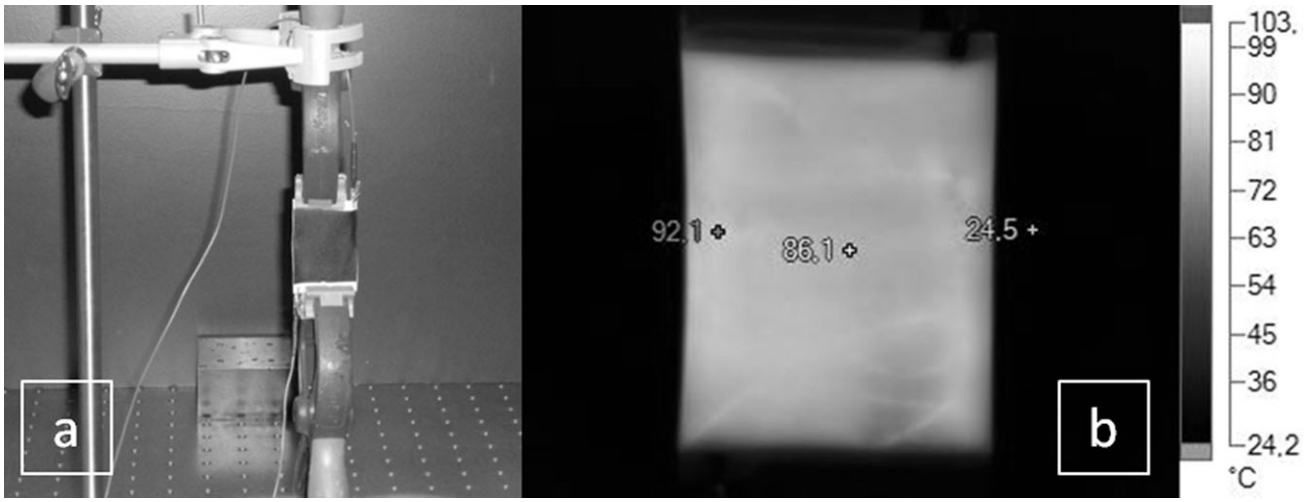

Figure 9. IR-thermography, (a) sample setting, (b) homogeneously heated sample.

energies of the substrates, which are listed in Table II. The adaptation of the initial formulation had an influence both on the viscosity and on the contact angle. Due to a modified proportion of solvent to polymer binder and the use of a conductive material, the contact angle was reduced and this, in turn, resulted in a better wetting. As a result of the formulation process, the surface tension of the CNT dispersions is reduced, as shown in Figure 3.

Surface Energies of the Substrates

The disperse fractions of fluids were calculated on the basis of correlations formulated by Owens, Wendt, Rabel, and Kaelble and by taking into account the contact angle measured on a non-polar PTFE surface[23]: eq. (1) σ_l^D for the disperse fraction of the liquid surface tension, σ_l for the overall surface tension of the liquid, σ_S^D for the disperse fraction of the substrate surface energy, and θ for the contact angle (see also Figure 2).

While the overall surface tension of Aquacyl dispersions decreased by reducing both the polar and the disperse fraction with the progress of the formulating, the decrease of the surface energy of FC dispersions was primarily due to a modification of the disperse fraction. The different dispersant systems of the manufacturers produced a different behavior of formulating and consequently of wetting solid surfaces (see Figure 3).

The different wetting behavior is also clearly shown in Figure 4. The measurement points of the formulations are, with the exception of FC23, below the 0°-wetting envelope for the substrate PC with a primer. Consequently, under ideal conditions, a complete wetting of the substrate by these formulations can be expected. The 0°-wetting envelope for PC does not include any of the formulations, a complete wetting is therefore not indicated for this case. Only the formulation AQ13 affects the PC wetting curve.

Printing. The printing tests were performed using the aforementioned equipment units and parameters. By means of dispersions AQ1 and FC2, it was not possible to produce a homogeneous, uniform multilayer system. Although the measuring point for AQ1 in Figure 4 is below the 0°-curve for PC with a primer and a surface wetting is carried out with the first printing pass, several overprints do not lead to the desired result in comparison with other formulations. Therefore, these two dispersions are not included in further analysis and evaluations.

With 20 layers printed on top of each other and under given material and process parameters, it was possible to realize an optimum relation of sheet resistance and layer adhesion with corresponding flexibility. As commercially available CNT dispersions are used for the production of printing inks, options for adjusting viscosity and solids content are limited. The maximum CNT content of a dispersion with appropriate properties for ensuring printability is presently not known. The dependence of the sheet resistance of printed CNT layers on the number of layers is described in Ref. 11 for textile substrates. Increasing the number of layers from 3 to 5 results in a decrease of sheet resistance by 55 times. However, if you increase the number of layers from 5 to 20, sheet resistance only decreases by six times. Sheet resistance behavior on a PC substrate is similar.

The color of the printed layer is black. The color density D was measured using a Techkon R410 densitometer. D is about 2.1 for

Table 3. Heating Rates

	AQ3	AQ35	AQ13	AQ12	FC23
dT/dt (RT→70°C) [K/s]	11	14.2	10.5	-	-
dT/dt (RT→67°C) [K/s]	-	-	-	6.7	-
dT/dt (RT→37°C) [K/s]	-	-	-	-	1.2

Applied Polymer SCIENCE

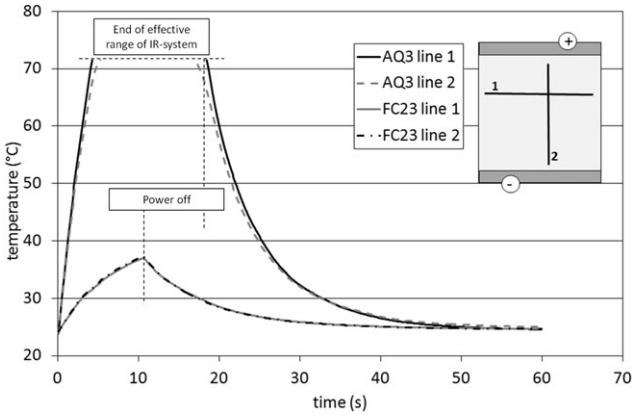

Figure 10. IR-thermography, temperature time curves of AQ3 and FC23 layers.

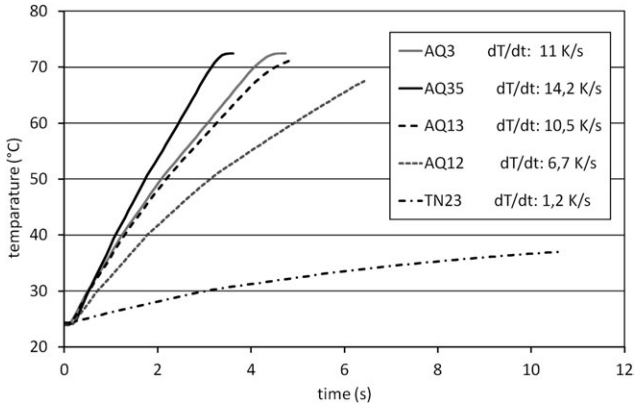

Figure 11. Highest heating rates of the printed CNT layers.

samples with 5, 8, 12, and 20 layers. The values cover the saturation range of the $D(s)$-characteristic (layer thickness s).

Characterization of Printed Layers

The layers are flexible and adhere very well. Macroscopically, no defects could be found. Homogeneous heating of the whole area indicates a printed layer free of cracks.

SEM images of CNT layers printed with various formulations AQ12, AQ13, AQ3, AQ35, and FC23 are shown in [Figure 5 (a–e)]. These layers consist of a network of CNTs with different lengths, diameters, and appearances. The CNTs of Aquacyl appear thicker in comparison to those of Future Carbon [see Figure 5(e)]. The high aspect ratio of the Aquacyl CNTs is clearly shown in Figure 5(f). In the edge region of a printed layer, the individual CNTs are unbound, with diameters in the double-figure nanometer range, where the lengths are between 2 and 4 μm. Any significant differences between the layers of various AQ formulations cannot be determined with the help of SEM images.

In Figure 6 the focused ion beam images of CNT-layers on a PC substrate are shown. Image (a) gives a view of the cross-section of the 2 μm-thick layer printed with formulation AQ3, and image (b) shows the 6 μm-thick FC23 layer. As shown, the FC23 thickness is three times the AQ3 thickness. Considering the mass load of the printed areas and the consequent sheet resistances and electrical power (Figure 6), differences between the layers printed with formulations made out of the dispersions of different manufacturers are evident. The FC23 mass load exceeds the AQ3 load by 40%. In spite of that, the electrical power of the printed AQ3-layers is nine-times the power of the FC23-layers, and the AQ3-sheet resistance is 23-times smaller than the FC23s. The complex interactions of the CNTs, dispersants, and binders reveal different property profiles comparing dispersions with the same CNT mass portions.

Masses of Prints Layers, Sheet Resistance, and Electrical Power. In Figures 7 and 8, the correlations between the parameters important for the characterization of printed CNT films are shown. It is obvious that an increase of solid content in the formulations, with the given surface printability, results in increasing surface masses of printed layers, decreasing layer resistance values, increasing electric power, and, as expected, higher heating rates can be achieved. This is the case when Aquacyl-based formulations are compared with each other. The printable formulation on the base of dispersion supplied by Future Carbon does not reflect the above mentioned tendencies in comparison to the Nanocyl formulations. Despite a relatively high surface weight, the values for the layer resistance are comparatively high and the electric power and the achievable heating rate are correspondingly lower. The aforementioned various changes in the properties of the dispersions during formulating (surface tension, density) and a different appearance of layers under the SEM are also apparently reflected in the performance values of the layers. The reasons for the differences should be searched for in the complex interaction of CNT properties (aspect ratio, number of tubes, type of CNT, functionalizations, etc…) and the dispersant system.

IR-Thermography. The samples of the printed layers with dimensions of 35 mm × 50 mm were provided with electrical contact strips of DuPont screen printing paste and connected via silver-plated terminal contacts with the voltage supply system. The sample freely suspended in the air on a laboratory stand, [see Figure 9(a)] was positioned in such a way that a defined distance to the IR camera system could be ensured. The emission coefficient was $\varepsilon \approx 0.95$. The data were collected at 50 Hz for 60 s. The ambient temperature was determined with a reference value of 24°C. The heating rates achievable by resistive heating are up to 14.2 K/s (see also Table III). In Figure 11 the sections of the temperature–time curves with the corresponding maximum heating rates are shown. The uniform heating of the sample surface

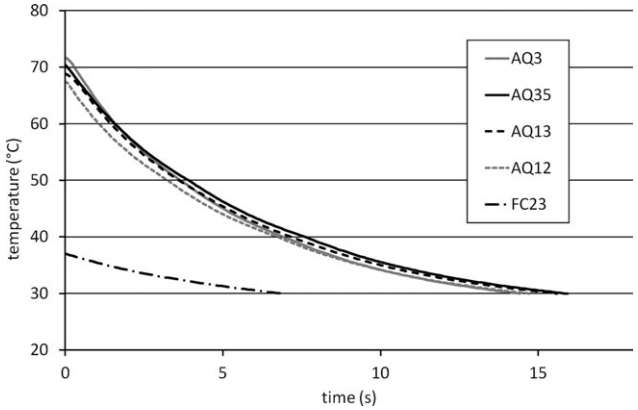

Figure 12. Cooling rates.

Table 4. Cooling Rates

	AQ3	AQ35	AQ13	AQ12	FC23
dT/dt (70°C→50°C) [K/s]	5.8	5.2	4.5	-	-
dT/dt (67°C→50°C) [K/s]	-	-	-	5.3	-
dT/dt (50°C→30°C) [K/s]	1.9	1.7	1.5	1.8	-
dT/dt (70°C→30°C) [K/s]	2.8	2.5	2.3	2.5	-
dT/dt (37°C→30°C) [K/s]	-	-	-	-	1

in Figure 9(b) can be regarded as the result of a good interaction between the CNT formulation, process parameters, and the substrate. The diagram in Figure 10 shows the temperature–time profile of printed CNT surfaces. The temperature measuring and evaluation are based on the orthogonal line scans; see the scheme at the top on the right. The curves of the temperatures above the scans 1 and 2 are nearly identical for the respective sample. This, in turn, can be regarded as an indication of the homogeneity of the printed layer and the temperature distribution. Printed samples of the formulations AQ3 and FC23, both with a solid content of 3% CNT, were compared. The plateau in the curve of the sample AQ3 results from the upper temperature limit of 75°C of the IR measurement system. The heating rates amount for AQ3 11 K/s in the monitored temperature range from room temperature to 70°C and for FC23 −1.2 K/s in the temperature range from room temperature to 37°C. The tests were carried out by means of an IR-thermographic camera. The voltage applied to the CNT surfaces was 12 V. Deformations of the samples occurred when temperature treatment of the uncooled substrate exceeded a critical period of time and not only the layer was heated, but also the substrate with a thickness of 100 microns itself.

The cooling behavior depends on the substrate and its heat capacity, the ambient temperature, the sample preparation, and the experimental setup. The cooling curves of the samples show, with the exception of FC23, a nearly identical shape. The diagram of Figure 12 shows the course of cooling from 70°C down to 30°C. The cooling took place in a period of about 15 s. For the FC23 samples, the temperature range of cooling was from 37°C down to 30°C. Table IV contains cooling rates for different temperature intervals, which might be of interest for applications.

CONCLUSIONS

It could be demonstrated that layers can be applied to the PC film using formulations based on commercially available, aqueous CNT dispersions and by means of flexographic printing that is suitable for mass volumes. The heating rates during resistive heating (12 V voltage applied; current measured) of these layers can amount, depending on the formulation, up to 14 K/s in the temperature range from room temperature to 70°C. The temperature–time curves were recorded with the help of an IR camera system. The cooling was very dependent on the substrate and could be actively supported or regulated. Possible applications can include lab-on-chip systems with injection-molding integration of printed CNT layers or electrodes in cyclic voltammetry systems. Dispersions from different manufacturers show different properties after formulation as well as the layers printed with these formulations. The reasons for the differences should be searched for in the complex interaction of CNT properties (aspect ratio, number of tubes, type of CNT, functionalizations, etc…) and the dispersant system. Therefore, there is enough potential for a targeted, application-specific setting of layer properties.

CREDITS

The experiments with the IR camera system were carried out at the University of Applied Sciences, Faculty of Automotive Engineering, Chair of Engineering Mechanics, headed by Professor Vogel. The SEM images were prepared at Fraunhofer ENAS Chemnitz.

REFERENCES

1. Huebler, A. C.; Hahn, U.; Beier, W.; Lasch, N.; Fischer, T. In 2nd International IEEE Conference on Polymers and Adhesives, Zalaegerszeg, **2002**; p 172.
2. Krucinska, I.; Skrzetuska, E.; Urbaniak-Domagala, W. *J. Appl. Polym. Sci.* **2011**, *121*, 483.
3. Sanchez, M.; Rincon, M. E. *Sens. Actuat. B* **2009**, *140*, 17.
4. Denneulin, A.; Bras, J.; Blayo, A.; Neuman, C. *Appl. Surf. Sci.* **2011**, *257*, 3645.
5. Song, J. W.; Kim, Y. S.; Yoon, Y. H.; Lee, E. S.; Han, C. S., Cho, Y.; Kim, D.; Kim, J.; Lee, N.; Ko, Y. G.; Jung, H. T.; Kim, S. H. *Phys E* **2009**, *41*, 1513.
6. Takenobu, T.; Miura, N.; Lu, S. Y.; Okimoto, H.; Asano, T.; Shiraishi, M.; Iwasa, S. *Appl. Phys. Express* **2009**, *2*, 025005.
7. Noh, J.; Jung, M.; Jung, K.; Lee, G.; Kim, J.; Lim, S.; Kim, D.; Choi, Y.; Kim, Y.; Subramanian, V. *IEEE Electron Device Lett.* **2011**, *32*, 638.
8. Ha, M.; Xia, Y.; Green, A. A.; Zhang, W.; Renn, M. J.; Kim, C. H.; Hersam, M. C.; Friesbie, C. D. *ACSNANO* **2010**, *4*, 4388.
9. Meyer K. H. Technik des Flexodrucks (Flexo Printing Technique); St. Gallen: Switzerland, Rek & Thomas Medien AG, **2006**.
10. Søndergaard, R. R.; Hösel, M.; Krebs, F. C. *J. Polym. Sci. Part B: Polym. Phys.*, **2013**, *51*, 16.
11. Fischer, T.; Wetzold, N.; Elsner, H.; Kroll, L.; Huebler, A. C. Nanomater. *Nanotechnol.* **2011**, *1*, 18.
12. Hu, L.; Hecht, D. S.; Grüner, G. *Chem. Rev.* **2010**, *110*, 5790.
13. Kang, T. J.; Kim, T.; Seo, S. M.; Park, Y. J.; Kim, Y. H. *Carbon* **2011**, *49*, 1087.

14. Yoo, H. J.; Kim, H. H.; Cho, J. W.; Kim, Y. H. *Surf. Interface Anal.* **2012**, *44*, 405.

15. Kim, D.; Lee, H. C.; Woo, J. Y.; Han, C. S. *J. Phys. Chem.* **2010**, *114*, 5817.

16. Pradhan, N. R.; Duan, H.; Liang, J.; Iannacchione, G. S. *Nanotechnology* **2009**, *20*, 245705.

17. Giannitsis, A. *Estonian J. Eng.* **2011**, *17*, 109.

18. Shaw, K. J.; Docker, P. T.; Yelland, J. V.; Dyer, C. E.; Greenman, J.; Greenway, G. M.; Haswell, S. *J. Lab Chip* **2010**, *10*, 1725.

19. http://www.electronics-cooling.com/2011/06/lab-on-a-chip-thermal-management-solutions/ (accessed June 11, 2012).

20. Lasance C.J.M.; Ponjee M. Lab-on-chip thermal management solutions *Biomicrofluidics* **2011**, *3*, 012005.

21. Wang, A.; Tolley, H. D.; Lee, M. L. *J. Chromatogr. A*, **2012**, *1261*, 46.

22. Peham, J. R.; Recnik, L.-M.; Grienauer, W.; Vellekoop, M. J.; Nöhammer, C.; Wiesinger-Mayr, H. Microsyst. *Technol.* **2012**, *18*, 311.

23. Ogonczyk, D.; Wegrzyn, J.; Jankowski, P.; Dabrowski, B.; Garstecki, P. *Lab Chip* **2010**, *10*, 1324.

24. On the move with innovation, http://www.materialscience.bayer.com/en/Challenges-and-Solutions/Mobility/Solutions.aspx, 2012 (accessed December 03, 2012).

25. CarboDis, http://www.future-carbon.de/downloads/Flyer_-CarboDis_v01_ 01_EN.pdf (accessed July 12, 2011).

26. AQUACYL 0301 *CarboDis*, Material Safety Data Sheet, July 15 2009, Revision No1.

27. Owens, D. K.; Wendt, R. C.*J. Appl. Polym. Sci.* **1969**, 13, 1741.

28. Cirlin, E. H.; Kaelble, D. H. *J. Polym. Sci. Polym. Phys. Ed.* **1973**, *11*, 785.